Channel Dynamics, Sediment Transport, and the Slope of Alluvial Fans: Experimental Study[1]

Kelin X. Whipple, Gary Parker,[2] Chris Paola,[3] and David Mohrig[2]

Department of Earth, Atmospheric and Planetary Sciences, Massachusetts Institute of Technology, Cambridge, MA, 02139

ABSTRACT

We present the results of an experimental study of alluvial fan sedimentation under conditions of constant inflow water discharge Q_w, sediment supply Q_{so}, and median grain size D. The study was designed to complement and test a recently formulated model of alluvial fan sedimentation and to emphasize the interactions between, and controls on, flow channelization and equilibrium fan slope. Flow channelization and fan sedimentation were studied under conditions of nearly steady, uniform aggradation. Steady conditions were achieved by imposing a steadily rising base level, just in balance with the average sediment aggradation rate. Experimental inflows covered a wide range of conditions, allowing examination of the effects of variations in Q_w, Q_{so}, and D in both bedload- and suspension-dominated environments. Experimental results were most consistent with an expanding-flow channel model. Key experimental findings successfully and quantitatively predicted by the expanding-flow theory include: (1) straight to slightly concave radial profiles of bedload-dominated fans; (2) distinctly convexo-concave profiles of suspension-dominated fans; (3) a strong, inverse relationship between Q_w and fan slope; (4) a strong, but secondary, relationship between Q_{so} and fan slope; and (5) near-independence of D and fan slope so long as transport stage is high and bedload transport dominant. However, potential scale effects in the experiments arose from reduced flow Reynolds numbers and incorrect geometric scaling of channel widths; no confident conclusions regarding the debate over the relative importance of ''sheetfloods'' and braided channel flows can be drawn from the experimental data. Extrapolation to field scale is best accomplished through appropriate application of the theoretical model herein confirmed against experimental data.

Introduction

The Problem. The controls on the size, slope, hydraulics, and sedimentary character of alluvial fans have long been debated by geologists and engineers (e.g., Bull 1977; French 1992; Whipple and Trayler 1996). Alluvial fans have a global distribution and form in a wide range of climatic and tectonic regimes wherever sediment-laden streams cross structural or topographic boundaries associated with a notable decrease in slope and lateral confinement and have been used as important indicators of (1) tectonic activity in the ancient record, (2) rates and timing of neotectonic deformation, and (3) climatic change. In addition, understanding the unique flood hazard on alluvial fans is increasingly important as urban development spreads into mountainous areas. Much research has been devoted to the problem of how fan slope is related to variables such as water discharge, sediment flux, and grain size, as well as how changes in fan slope manifested in segmented profiles or fan-head trenches might be controlled by changes in these variables or intrinsic process thresholds (Blair 1987; Blissenbach 1954; Bull 1977; Denny 1965; Hooke and Rohrer 1979; Nilsen and Moore 1984; Rachochi 1981; Schumm et al. 1987). Random-walk and statistical Markov-chain models have reproduced patterns of long-term shifting of deposition resulting in the construction of fan lobes (Hooke and Rohrer 1979; Price 1976; Schumm et al. 1987). However, no mechanistic theory of alluvial fan flooding and sedimentation has emerged. As a result, quantitative predictions of how fan slope will respond to climatic or tectonic forcings have not been possible. Indeed, even the relative importance of water discharge, sediment flux, and grain size to fan slope has not been clearly established. Relatively uncon-

[1] Manuscript received August 12, 1997; accepted July 14, 1998.

[2] St. Anthony Falls Laboratory, University of Minnesota, Minneapolis, MN, 55414.

[3] Department of Geology and Geophysics, University of Minnesota, Minneapolis, MN, 55454.

[The Journal of Geology, 1998, volume 106, p. 677–693] 0022-1376/98/10606-0001$01.00

fined, divergent flows, rapid backfilling and shifting of channels, the importance of infrequent, high transport stage events and a paucity of field and experimental data on alluvial fan flood hydraulics all contribute to this lack of quantitative understanding.

Approach and Scope. In this paper we present the findings of the experimental phase of a combined experimental, field and theoretical study of alluvial fans. The theoretical development is presented by Parker et al. (1998*a*), and applications to field problems of engineering interest are discussed in Parker et al. (1998*b*). In this series of papers we seek to quantify the relationships among fan morphology, flow channelization, and boundary conditions such as volume water discharge (Q_w), volume sediment input rate (Q_{so}), and grain size (median size D). Here we extend earlier, more qualitative laboratory studies (Bryant et al. 1995; Hooke 1967; Hooke and Rohrer 1979; Schumm et al. 1987) by (1) controlling base level conditions to achieve quasi-steady-state aggradation, (2) maintaining direct control of all boundary conditions, (3) considering a wider range of input variables (Q_w, Q_{so}, D), (4) performing a more extensive analysis of scaling relationships between the model and field prototype, and (5) analyzing and interpreting our experimental data in the context of a mechanistic theoretical model (Parker et al. 1998*a*).

Scale-model laboratory studies such as this (e.g., Bryant et al. 1995; Hooke 1967; Hooke and Rohrer 1979; Schumm et al. 1987) and field studies on artificial alluvial fans (e.g., Parker et al. 1998*b;* Rachochi 1981) allow the investigator to: (1) circumvent logistic difficulties in field studies of alluvial fan sedimentation, and (2) eliminate complications associated with rapidly varying external forcings such as flood discharge and sediment supply. Naturally these advantages are offset by limitations. The greatest limitation of the present study is that we consider only the idealized case of constant inflow conditions (Q_w, Q_{so}, and D). The important question of the dominant discharge on fans subjected to natural variations in stream hydrographs and sediment supply discussed by Hooke and Rohrer (1979) is a step beyond the scope of the present paper, which should nevertheless provide an appropriate baseline for its future investigation. In addition, certain unavoidable scale effects may influence the behavior of flows and sediment transport on scale-model fans. Extrapolation to field scale is most effectively done through application of theoretical models in which any scale effects can be accounted for directly (e.g., Parker et al. 1998*a,* 1998*b*).

Theoretical Framework

The theoretical model of Parker et al. (1998*a*) predicts slope profiles of radially symmetrical (one-dimensional) alluvial fans with angle of expansion θ (figure 1) under conditions of uniform, steady-state aggradation. The analysis pertains to constant water discharge Q_w, volumetric sediment inflow rate Q_{so}, and uniform grain size D. The effect of varied discharge and sediment supply is introduced in a simple way by means of an assumed intermittency of flow. That is, the constant flow is assumed to be turned on for fraction I of time; otherwise it is completely turned off (Paola et al. 1992). Losses of water due to infiltration are neglected. To achieve an analytical solution, channels are necessarily treated as time- and space-averaged flow configurations (averaged over several avulsion cycles and along a line of constant radius across the fan surface). The theory accommodates two end-member channel configurations: (1) unchannelized, expanding flow (akin to sheetfloods), and (2) a distributary network of equilibrium or self-formed channels, following Parker (1978*a*) and Paola et al. (1992).

The channelization rule determines how the total "effective" width of channels varies with distance down fan. For the equilibrium channel case it is assumed that channel width is adjusted to achieve bank stability during active sediment transport. This condition equates to the develop-

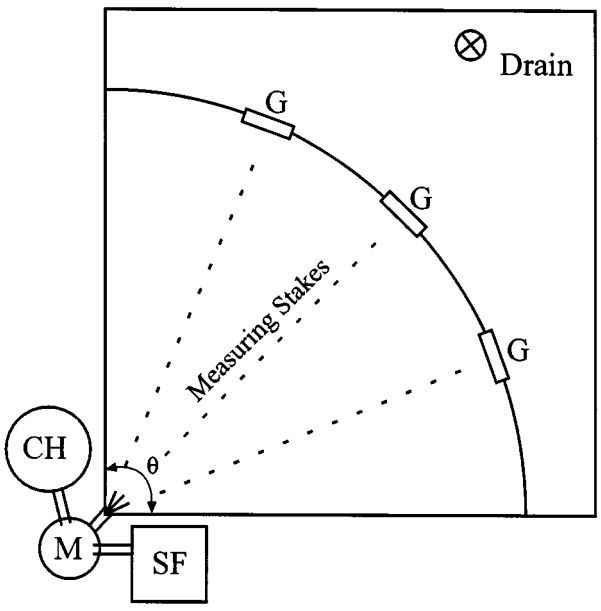

Figure 1. Schematic of experimental basin design showing constant head tank (CH), sediment feeder (SF), mixing funnel (M), weir gates (G), and fan expansion angle θ.

ment of a channel system with spatially constant Shields stress, τ^*, as is often observed in gravel-bedded, braided channels (Parker 1978*a,* 1978*b*). Diffusion-based sediment transport models familiar in the basin analysis literature are predicated on the equilibrium channel assumption (e.g., Begin 1988; Flemings and Jordan 1989; Paola et al. 1992).

Given the assumption that the channels can indeed be modeled as ''average'' or ''effective'' flow configurations using one of the above channelization rules, the theoretical model simply combines conservation of mass for water and sediment, conservation of momentum, a standard hydraulic resistance relationship (Manning-Strickler or Chezy) and a generalized sediment-transport equation (Parker et al. 1998*a*). Momentum conservation is satisfied in terms of steady, uniform flow in the ''effective'' channel. Parker et al. (1998*a*) show that analytical expressions can be written for the equilibrium slope of an alluvial fan as a function of volume sediment influx Q_{so}, water discharge Q_w, median grain-size D, and the following set of dimensionless parameters: a coefficient α_r and exponent p describing hydraulic resistance; a coefficient α_s, an exponent n and a critical Shields stress τ_c^* describing sediment transport; a submerged specific gravity R of the sediment; and coefficient χ or α_b governing flow channelization.

Parker et al. (1998*a*) show that in the case of simple expanding flow these relations reduce to the following forms for the variation of the width of the ''effective'' channel B_{ac} and the mean down-fan bed slope S in radial distance r:

$$B_{ac} = \chi\theta r \tag{1a}$$

$$S = \left\{R\left[\left(\frac{1}{\alpha_s}\frac{Q_{so}(1-\hat{r}^2)}{\sqrt{RgD}D\chi\theta r}\right)^{1/n} + \tau_c^*\right]\right\}^{(3+2p)/(2+2p)} \times \alpha_r^{1/(1+p)}\left(\frac{Q_w}{\sqrt{gD}D\chi\theta r}\right)^{-1(1+p)}, \tag{1b}$$

where $\hat{r}$ is dimensionless down-fan distance ($\hat{r} = r/L$), L is fan length, and g is gravitational acceleration. Note that χ corresponds to the fraction of fan width occupied by water, a parameter that would be expected to vary with Q_w (and perhaps Q_{so} and D). Similarly, in the case of equilibrium braided channels these relations are shown to reduce to:

$$B_{ac} = D\alpha_s^{-1}\left(\frac{Q_{so}(1-\hat{r}^2)}{\sqrt{RgD}D^2}\right)\left(\frac{\alpha_b}{R} - \tau_c^*\right)^{-n} \tag{2a}$$

$$S = \left[R^{-1/2}\alpha_s^{-1}\alpha_b^{(3+2p)/2} \times \alpha_r\left(\frac{\alpha_b}{R} - \tau_c^*\right)^{-n}\left(\frac{Q_{so}(1-\hat{r}^2)}{Q_w}\right)\right]^{1/(1+p)} \tag{2b}$$

Note that (2a) implies that, in the case of equilibrium braided channels, the effective width of active channels B_{ac} is not expected to vary with Q_w. Rather, fan slope is the variable expected to adjust, fully compensating for any change in water discharge, as seen from (2b). This same behavior is expected for diffusion-based sedimentation models.

The expanding flow scenario is akin to alluvial fan ''sheetflooding'' described in the literature (e.g., Blair and McPherson 1994), but is distinct in that it neither implies that the entire fan is inundated nor that the flood is characterized by a uniform flow depth. Rather it states that the total width of inundation, including all channels and zones of unconfined flow, increase linearly with distance down fan. The expanding flow model is incomplete as the fractional flow width parameter χ cannot be predicted a priori. The equilibrium channel model is more physically satisfying, as all parameters are predicted from theory, but it is not immediately clear that equilibrium channels have time to develop in the rapidly avulsing, high transport stage, high discharge experimental flows or that they are necessarily representative of typical alluvial fan floods (e.g., Blair 1987; Blair and McPherson 1994; Rachochi 1981). Testing theoretical predictions against experimental data requires determination of which channelization rule best captures observed flow conditions. Extrapolation of these results to the field requires careful consideration of potential scale effects.

Experimental Design

Facility. Two experimental basins were used in this experimental program. The two basins differed in size but had essentially the same design. Preliminary experiments were conducted in a 2.1 m quarter-circle ($\theta = 90°$) basin (figure 1). Subsequently, a 5.2m basin with an expansion angle of 67.5° was constructed and additional experiments were carried out using both basins. The wedge-shaped geometry of the experimental basins was chosen as a rough approximation of the geometry of fans laterally restricted by adjacent, coalescing fans. In addition, this geometry imposed a simplifying axial symmetry, allowing direct comparison with the

(one-dimensional) theoretical treatment in Parker et al. (1988 *a*). The natural asymmetry commonly observed in unrestricted fans and discussed by Hooke and Rohrer (1979) is not addressed here.

The outer perimeters of both basins were fitted with one or more adjustable weir gates to allow precise control of base level (figure 1). In all experiments a constant head tank with adjustable sleeves was used to supply steady water discharges Q_w ranging from 108 to 475 cm^3s^{-1}. Steady sediment supply rates Q_{so} ranging from 1.73 to 15.09 cm^3s^{-1} were delivered by an auger-type dry sediment feeder. Water and sediment inputs were mixed in a funnel before being delivered to the apex of the basin, either through a flow splitter (2.1 m basin) or through a 10-cm wide inlet channel (5.2 m basin). In addition, a second constant head tank was set up to allow periodic addition of a constant concentration of colored dye to the inflow, to aid photographic documentation of flow configuration.

Data collected during the experiments included the topographic evolution of the fan surface, the spatial and temporal evolution of flow configuration (channels and zones of expanding flow), and occasional spot measurements of flow width, depth, and surface velocity (used to define approximate flow Reynolds numbers). Radial topographic profiles were measured periodically by taking readings on three lines of ruled stakes spaced 15 cm apart in the beds of the experimental basins (figure 1). For monitoring complex and rapidly shifting flow patterns, the basins were fitted with overhead still and video cameras. All data were collected without interrupting the experiments.

Experimental Protocol. Weir gates at the basin margin were operated to control the elevation of ponded water at the distal end of the experimental basins. In all experiments the weir gates were initially set to hold 1–2 cm of ponded water, and the experimental fans were deposited as fan deltas (henceforth called ''fans'' for simplicity). Delta fronts were maintained as abrupt margins, and the ponded water had little effect on fan sedimentation beyond the desired role of base level control. During each experiment, sediment size D, input sediment flux Q_{so}, and input water discharge Q_w were held constant. In the initial phase the fan was allowed to prograde across the basin under conditions of constant base level. Once the fan had reached the desired maximum size L (2 m in the small basin and either 4 or 5 m in the large one), the weir gates were raised incrementally to impose a constant rate of base level rise chosen to maintain the position of the delta front, just trapping all sediment within the basin. The rate of base level rise was thus chosen to approximate the mean surface aggradation rate v_s, computed directly from known input conditions and basin geometry (Parker et al. 1998*a*). Within a relatively short time after the imposition of a constant rate of base level rise, the mean radial profile of the fan approached a state of steady, uniform aggradation in precise analogy to a balance between aggradation and subsidence over geologic time (e.g., Paola et al. 1992; Gordon and Heller 1993; Whipple and Trayler 1996).

During the experiments radial topographic profiles were recorded at regular time intervals chosen to allow <0.5 cm of average bed level rise between measurements. After the initial progradation of the fan to the desired length, input conditions (Q_w, Q_{so}) were held constant until the condition of uniform, steady-state aggradation had been at least approximately achieved (as documented in 2–3 bed-elevation readings with unchanging slope profiles). Typical times to this state varied from 2 to 30 hr, depending on the size of the fan, the sediment feed rate Q_{so}, and the water discharge Q_w. Photographic documentation of channel patterns concentrated on these periods of nearly steady, uniform aggradation, and input conditions were held constant for long enough to allow channels to sweep the entire fan surface. The mode (still vs. video) and frequency at which images of the flow configuration were obtained varied greatly between experiments (from still photographs taken every 30 minutes to continuous video recording) as our laboratory protocol evolved over the 2 yr period of the study. Once the photographic survey was completed, input conditions were changed (either Q_w or Q_{so}) and maintained until quasi-steady-state was re-established. Typically either Q_w would be decreased or Q_{so} increased between experiments, leading to a steepening of the fan surface.

Experimental Materials and Conditions. Experimental fans were built using a wide range of input conditions (Q_w, Q_{so}) and sediment types (various median sizes D, unimodal and mixed size distributions, quartz sand and silt, and crushed coal). Results from a total of 51 individual experiments, comprising 17 experimental runs, and grouped into five thematic run series are reported here. Materials used and conditions tested are summarized in table 1. Each run series addressed a different scientific objective (e.g., dependence of fan slope on Q_w and D), or a different type of fan system (e.g., suspension-dominated vs. bedload-dominated fans). Series 1 and 2 concerned suspension-dominated systems using quartz sand and fine crushed silica as model sediment. Within Series 1 and 2 Runs S2, S7, and S9 were transitional from suspension- to bedload-

Table 1. Experimental Conditions

Series	Objective	Run	Basin	R	D_{50} (μm)	σ_g	Q_w (cm^3/s)	Q_{so} (cm^3/s)	Ave Slope	+/−
1	Suspension-dominated: runs with variable Q_w and D									
		S4	2.1	1.65	70	1.34	475	7.55	.045	.010
							230	7.55	.048	.009
							120	7.55	.091	.013
		S8	2.1	1.65	70	1.34	466	7.55	.031	.012
							225	7.55	.055	.007
							122	7.55	.072	.008
		S5	2.1	1.65	100	3.13	475	7.55	.042	.008
							230	7.55	.069	.004
							120	7.55	.099	.007
		S3	2.1	1.65	110	1.23	475	7.55	.047	.010
							230	7.55	.055	.010
							120	7.55	.089	.006
		S10	5.2	1.65	120	1.40	465	7.55	.054	.002
							230	7.55	.075	.002
		S2	2.1	1.65	160	1.36	475	7.55	.055	.008
							230	7.55	.098	.010
							120	7.55	.110	.010
		S7	2.1	1.65	160	1.36	475	7.55	.052	.005
							230	7.55	.082	.005
							120	7.55	.124	.010
2	Suspension-dominated: runs with variable Q_w and Q_{so}									
		S10	5.2	1.65	120	1.40	230	3.77	.060	.002
							120	3.77	.093	.002
							465	15.09	.065	.001
							230	15.09	.093	.001
		S9	2.1	1.65	160	1.36	225	3.77	.057	.006
							225	7.55	.084	.007
							225	15.09	.107	.010
3	Bedload-dominated: runs with variable Q_w and D									
		S12	2.1	1.65	270	1.45	465	7.55	.055	.005
							230	7.55	.087	.005
							120	7.55	.130	.009
		S13	2.1	1.65	460	1.62	465	7.55	.058	.004
							230	7.55	.086	.004
							120	7.55	.125	.005
		S1	2.1	1.65	550	1.37	230	7.55	.100	...
4	Suspension-dominated (coal): runs with variable Q_w and D									
		C2	5.2	.50	550	1.65	321	2.77	.015	.001
							267	2.77	.018	.001
							214	2.77	.023	.001
							160	2.77	.029	.001
		C3	5.2	.50	550	1.65	419	2.77	.016	.001
							214	2.77	.024	.001
		C4	5.2	.35	125	1.62	419	2.77	.008	.001
							321	2.77	.009	.001
							214	2.77	.013	.001
							108	2.77	.025	.001
		C5	5.2	.38	130	2.23	419	3.45	.009	.001
							321	3.45	.010	.001
							214	3.45	.014	.001
							108	3.45	.023	.001
5	Suspension-dominated (coal): runs with variable Q_{so}									
		C7	5.2	.38	130	2.23	214	1.73	.009	.001
							214	3.45	.013	.001
							214	6.90	.017	.003

dominated. Series 3 concerned bedload-dominated systems using quartz sand as model sediment. Problems with seepage losses to groundwater in the run with well-sorted medium sand (S1) prompted us to mix a small fraction of silt and fine sand into the medium sand to reduce hydraulic conductivity of the sediment (Run S13). Series 4 and 5 were concerned primarily with suspension-dominated systems using crushed coal as model sediment. The crushed coal experiments were designed specifically to model the upper portion of a field-scale man-made fan (Parker et al. 1998*b*). The lower density of crushed coal (R = 0.35–0.50) permitted Froude scale modeling of finer-grained prototype systems than was possible using quartz sand and silt as a model sediment (see below and Appendix A; Appendix A is available from *The Journal of Geology* free of charge upon request). Runs C2 and C3 with the 550 μm coal sediment were bedload-dominated.

Acceptable Froude-Scale Prototypes. In discussing scale relations, it is useful to introduce four dimensionless numbers: the Froude number, F_r, the Reynolds number, R_e, the Shields stress, τ^*, and the Rouse number, R_o. The numbers can be defined as follows: $F_r = U/(gH)^{1/2}$, $R_e = UH/\nu$, $\tau^* = u_*^2/(\rho RgD)$, $R_o = w_s/(\kappa u_*)$ where U denotes a characteristic velocity, H denotes a characteristic depth, ν denotes the kinematic viscosity of water, u_* denotes a characteristic shear velocity, ρ is water density, w_s denotes sediment fall velocity in quiescent water (see Dietrich 1982) and κ denotes the Karman constant (κ = 0.4). Similarly between model and field prototype in any dimensionless number is achieved when the number has the same values in the model as in the prototype.

Using the guidelines presented in the Graf (1977) and French (1985) and the scaling relationships given in Appendix A, acceptable Froude-scale prototype equivalents of the experimental fans can be determined. That is, field conditions approximately representative of the experimental runs can be delineated. Experiments in run series 3, with quartz sand model sediment ($160 \leq D \leq 550$ μm), were effectively bedload-dominated ($R_o > 1.5$) in both overbank and channel flows. However, for several of the experimental run series (Series 1, 2, and 5; table 1) active sediment transport processes included both bedload-dominated sheetflows and suspension-dominated channel flows. For the experiments using finer sediment sizes as well as crushed coal, Rouse numbers R_o remained below unity even in shallow sheetflows, suggesting suspension-dominated systems. However, greatly reduced Reynolds numbers in overbank sheetflows ($R_e < 200$, as compared to a value of ~500 marking the onset of turbulence in open channel flow) inhibited suspension, and thus in some cases unchannelized flows remained bedload-dominated. Conversely, channelized flows were fully turbulent ($R_e \sim 2000$), and vigorous suspension was observed. This transition between bedload and suspended load transport complicates the interpretation of experimental findings of some of the experiments in Run Series 1, 2 in terms of field-scale phenomena.

With the above caveats and relations in mind, admissible Froude-scale prototypes of our experimental fans include: (1) small (L = 500 m), steep (bed slope S = 0.07–0.15), coarse-grained (D = 18–138 mm) alluvial fans subjected to large flood discharges (Q_w = 100–400 m^3/s) and high sediment supply rates (Run Series 3: bedload-dominated sand experiments); (2) small (L = 500 m), moderately steep (S = 0.04–0.09), sand–fine gravel (D= 2–8 mm) alluvial fans subjected to large flood discharges (Q_w = 100–400 m^3/s) and high sediment supply rates (Run Series 1 and 2: suspension-dominated sand experiments); and (3) the upper part (L = 500 m) of large, gently sloping (S = 0.005–0.01), fine-grained (D = 0.1–0.5 mm) alluvial fans subjected to low flood discharges (Q_w = 8–10 m^3/s) and moderate sediment supply rates (Run Series 4 and 5: crushed coal experiments).

Observed Flow, Sediment Transport, and Deposition Phenomena

Overall Fan Development. The laboratory fans exhibited many of the distinctive characteristics of natural alluvial fans. These included straight to gently concave radial profiles, the occurrence of both the expanding flow and braided channel flow configurations, and rapid changes in flow paths associated with frequent channel avulsions. Despite (or because of) the complex flow-channelization history, the overall evolution of the fan surface followed a simple path, punctuated by occasional transients associated with major changes in flow configuration. During the initial progradational stage, the proto-fan quickly achieved an ''equilibrium'' slope maintained as the fan-wedge advanced steadily across the basin. Greater degrees of channelization in experiments with finer sediments led to a pulsating advance and a more convolute delta front. This pattern of progradation of a wedge of unchanging slope was repeated after each change in experimental conditions as the fan adjusted to a new equilibrium slope (figure 2). Transient profiles thus resembled the ''segmented'' fans described by Bull (1977), Hooke (1967), and others.

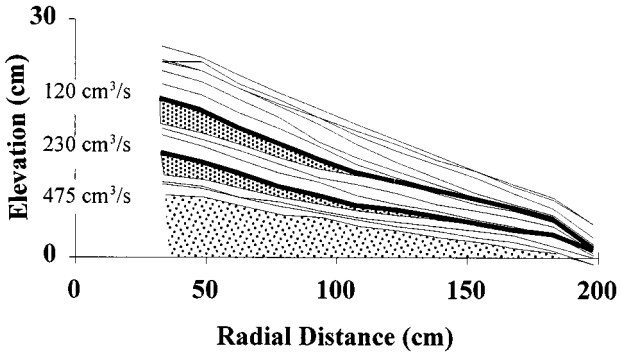

Figure 2. Pattern of fan-wedge progradation. Initial fan wedge (light dots) progrades with constant base level. Timelines (thin lines) show development of steady-state aggradation. Heavy lines indicate timelines immediately after a step decrease in water discharge (indicated on figure). Medium dot patterns highlight fan wedges produced by this change in discharge.

Once the entire fan was re-graded to the new sediment and water inflow conditions, and sediment again began reaching the delta front, the state of quasi-steady surface aggradation in pace with the rate of base level rise was reestablished (figure 2). In detail, and particularly on the suspension-dominated fans, the slopes of radial profiles fluctuated—with incision in proximal areas, and rapid aggradation in distal areas—as zones of flow concentration formed, entrenched, and back-filled (figures 3 and 4). However, the time- and space-averaged slopes of the experimental fans varied systematically with sediment size, water discharge, and sediment feed rate.

Channel Dynamics, Fan-Lobe Deposition, and Bedforms. In all experiments, flow varied in both space and time between one closer to expanding sheetflow and one closer to distinctly channelized braiding (e.g., figure 3). Channel behavior, including sudden avulsion, formation of channel-lobe couplets, backfilling of channels, and spontaneous formation of fan-head trenches (figures 3, 4, and 5) was similar to patterns described by Schumm et al. (1987) on the basis of their experiments on fluvial fans. Down-fan changes in flow configuration were pervasive and varied. Although flow was at times entirely unconfined right from the fan apex, such sheetflows were unstable, as anticipated in theoretical work on channel initiation (Izumi and Parker 1995; Loewenherz-Lawrence 1994; Smith and Bretherton 1972). Because of this instability, flow concentrations (channels) would form either after a short distance down fan, or after a short time immediately at the apex. Channels at times formed on all parts of the fan, with the deepest flows occurring

A

B

Figure 3. Photographs of typical channel-lobe couplets in flow configuration taken 30 min apart during run S9. Glare is from reflection of overhead lights. *A.* Flow configuration at runtime 1:55. *B.* Flow configuration at runtime 2:20.

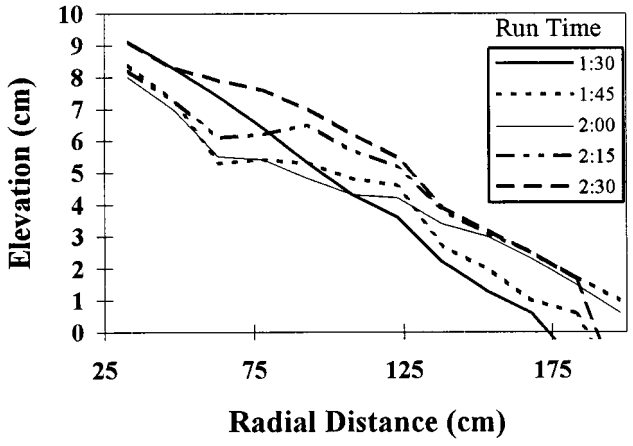

Figure 4. Centerline radial profiles recorded during the interval of time captured in the photographs in figure 3. Various line types indicate channel bottom profiles recorded at 15 min intervals. Rapid incision and subsequent backfilling is clearly visible.

near the fan head. These flow concentrations grew rapidly through incision and headward propagation, transporting large amounts of sediment to depositional lobes that form immediately downstream of channels (figure 5). Typical flow configurations consisted of short-lived paired couplets of flow concentrations (channels) in the incising reach and rapid flow expansions in the aggrading reach (figures 3, 4, and 5). As illustrated in figure 5, depositional centers migrated up-fan, resulting in a gradual backfilling of the recently formed channel; this incision-backfilling cycle recurred over a wide range of scales and on all parts of the experimental fans.

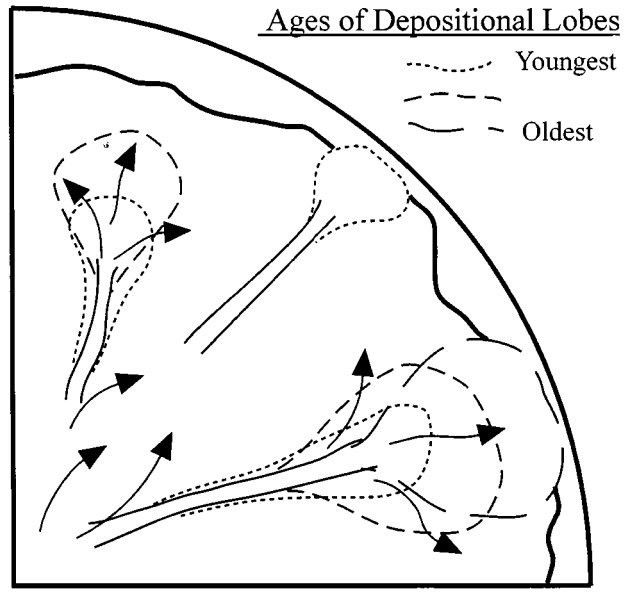

Figure 5. Schematic illustration of typical flow configuration, with a number of channel-lobe couplets characterized by rapidly expanding flow over the depositional lobe.

Average Depositional Slopes. Experimental fans exhibited straight to weakly concave (bedload-dominated systems) or convexo-concave (suspension-dominated systems) radial profiles (e.g., figure 2). Average depositional slopes were determined via least squares regression through truncated, spatially (three radial profiles) and temporally (two to three realizations during quasi-steady aggradation) averaged elevation profiles. Truncation of the upper and lower 10–15% of elevation profiles was required due to rapid elevation fluctuations near the fan apex, and short-term advance and retreat of the delta front. In the suspension-dominated sand and silt (70 μm $< D <$ 160 μm) experiments, fan slope is inversely correlated with Q_w and positively correlated with Q_{so} and D (figure 6*a, b*; table 1: Series 1 and 2). Generally, the observed variation with Q_w was the strongest and that with D the weakest. Data from a single run using a poorly sorted sediment mixture (D_{50} = 100 μm; run S5 on table 1), although not plotted along with the uniform-sediment experimental data in figure 6*a,* showed similar behavior.

Experimental data plotted for the 70 and 160 μm sediment sizes are averages of data from pairs of replicate runs (S4–S8 and S2–S7 for the 70 μm and 160 μm fans, respectively). Data from the replicate runs are reported with approximate error bars for comparison in figure 7, which show scatter characteristic of experiments in the 2.1-m basin (table 1; figure 4), but generally reproducible trends. Error bars represent the full range of slope variation over two to three realizations along three radial profiles. Experiments in the larger basin and with coarser model sediments showed significantly less temporal variability (table 1).

Similar to the suspension-dominated systems, slopes of bedload-dominated experimental fans are inversely correlated with Q_w (figure 8). However, as anticipated in the theoretical model of Parker et al. (1998*a,* 1998*b*), the bedload-dominated systems show a markedly different behavior as regards sediment size: the slope of experimental fans is largely independent of grain size (figure 8). Although this result may initially seem counter-intuitive, the theoretical model (see equation 1b) clearly predicts this behavior for the case of bedload transport (n = 1.5), constant friction factor (p = 0), and high excess shear stresses ($\tau_b \gg \tau_c^*$) (see equation 1 and development in Parker et al. 1998*a*). Note that in cases where critical Shields stress (τ_c^*) becomes im-

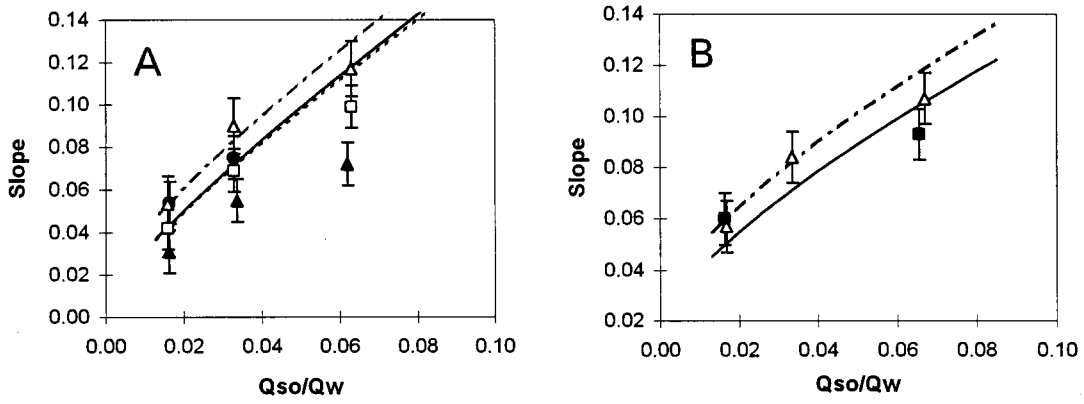

Figure 6. Fan slope as a function of sediment concentration (Q_{so}/Q_w) and sediment size (D) for the suspension-dominated fan experiments. Symbols for data series: 160 μm (open triangles); 120 μm (solid circles); 100 μm (open squares); 70 μm (solid triangles). Error bars represent variation in observed fan slopes. Lines are theoretical relationships described in the text (see equation 1 and table 2). Line types for theoretical curves: 160 μm (dash-dot); 120 μm (solid); 70 μm (dash). *A.* Experiments with water discharge as the independent variable (Series 1). *B.* Experiments with sediment supply rate as the independent variable (Series 2).

portant, the theory predicts (Parker et al. 1998*a*) and experiments confirm (Hooke 1968; Hooke and Rohrer 1979) a strong dependence on sediment size. The direct grain-size dependence seen in the fine sand and silt runs (figure 6*a*) is more difficult to explain and may in part be due to scaling problems with the fine grained sediments, as described below. The transition from grain-size dependent to grain-size independent behavior in our experiments is abrupt and occurs at about 160 μm.

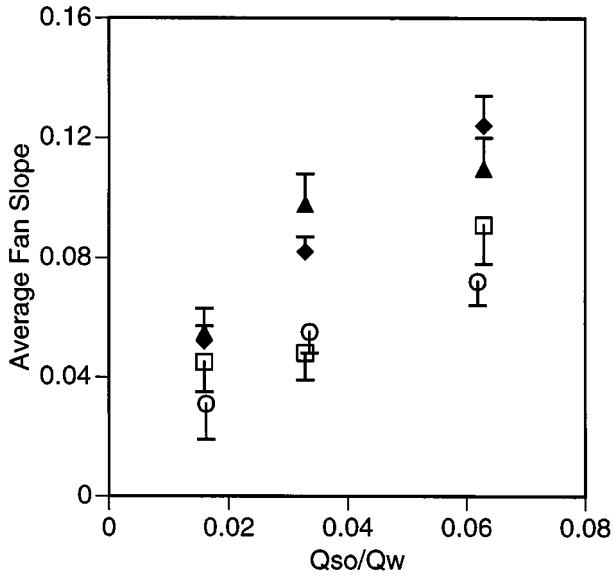

Figure 7. Reproducibility of measured fan slopes in the small basin (2.1 m) for the suspension-dominated fans. Symbols for data series: 70 μm, run S4 (open squares); 70 μm, run S8 (open circles); 160 μm, run S2 (solid triangles); 160 μm, run S7 (solid diamonds). Only half-error bars are plotted for readability. These data represent a "worst case" scenario because spatial and temporal variations in fan slope were strongest in the suspension-dominated experiments, and least constrained in the small basin (see table 1).

Results of the experiments with crushed coal model sediment (Series 4 and 5, table 1) are generally consistent with those involving sand and silt but quantitatively different (figure 9). For instance, fan slope is observed to increase more rapidly with decreasing water discharge. In addition, although a relatively strong grain-size dependence is apparent, appropriate sediment was available in only two distinct size classes (table 1) and little inference about this relationship is possible. Runs C2 and C3 with the 550 μm coal sediment were observed to be bedload-dominated, whereas the coal runs with $D \leq$ 130 μm were suspension-dominated; the grain size at which the transition from suspension-dominated to bedload-dominated transport occurs is unknown. Moreover, while a transition from grain-size dependent to grain-size independent behavior would be expected from theory, whether it occurs in these experiments is likewise unknown.

Analysis: Theory and Observation

Flow Channelization. Repeat photographic documentation of flow configurations allowed quantitative assessment of spatial and temporal variations in active flow width that can be used to constrain the channel configuration rule required for application of the theoretical model. In addition to the rapid temporal fluctuations in flow configuration observed in all experiments, significant differences in average flow conditions associated with differ-

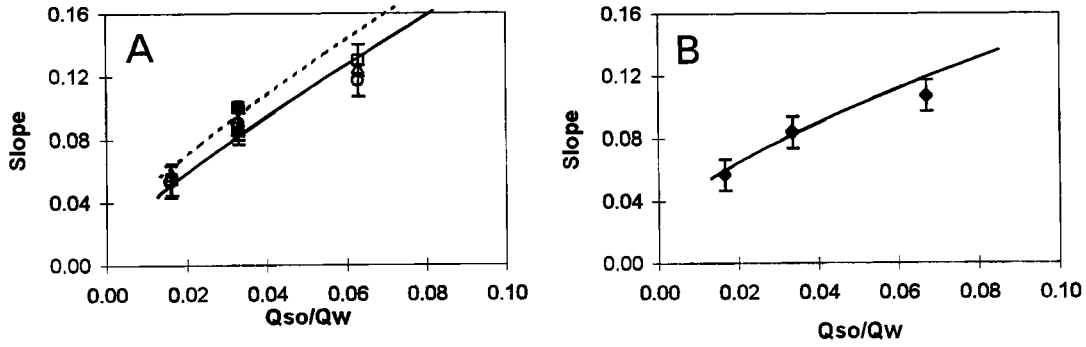

Figure 8. Fan slope as a function of sediment concentration (Q_{so}/Q_w) and sediment size (D) for the bedload-dominated fan experiments. Error bars represent variation in observed fan slopes. Lines are theoretical relationships described in the text (equation 1) computed with parameter values in table 2. *A.* Experiments with water discharge as the independent variable (Series 3). Symbols for data series: 550 μm (solid square); 460 μm (open triangles); 270 μm (open squares); 160 μm (open circles). Line types for theoretical curves: 550 μm, Q_w variable (dash); 270 μm, Q_w variable (solid). *B.* Experiment with sediment supply as the independent variable (Run S9). Data series: 160 μm (solid diamonds). Theoretical curve: 160 μm, Q_{so} variable (solid). Note that experiments with the 160 μm sediment were transitional from suspension to bedload-dominated.

ences in water discharge and sediment size were observed. Somewhat surprisingly, little variation in average active channel width occurred in response to changes in sediment feed rate, despite the concomitant change in fan slope. We consider, first, temporal fluctuations in flow channelization under steady conditions, and then explore the sensitivity of average flow configuration to variation in water discharge Q_w, sediment feed rate Q_{so}, and median grain size D.

Still photographs documenting channel configuration were obtained at five minute intervals over a one hour and fifteen minute period of steady-state aggradation during Run S10 (Q_w = 465 cm^3/s, Q_{so} = 7.55 cm^3/s, D = 120 μm sand). Flow widths were digitized and summed along five evenly spaced, concentric arcs. These data, reported as fractional

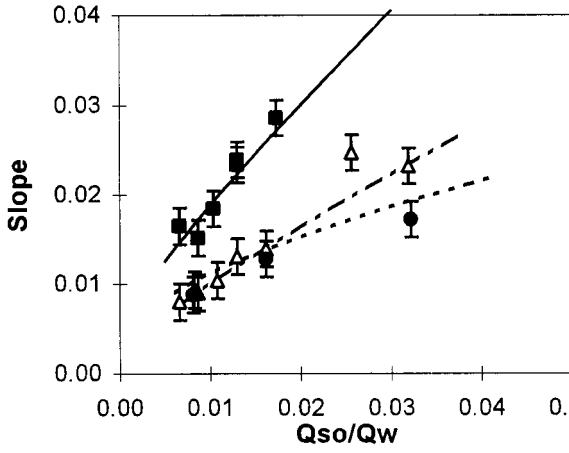

Figure 9. Fan slope as a function of sediment concentration (Q_{so}/Q_w), and sediment size (D) for the suspension-dominated crushed-coal fan experiments (Series 4 and 5). Symbols for data series: 550 μm, Q_w variable (solid squares); 130 μm, Q_w variable (open triangles), 130 μm, Q_{so} variable (solid circles). Error bars represent variation in observed fan slopes. Lines are theoretical relationships described in the text (equation 1) computed with parameter values in table 2: 550 μm, Q_w variable (solid); 130 μm, Q_w variable (dash-dot), 130 μm, Q_{so} variable (dash).

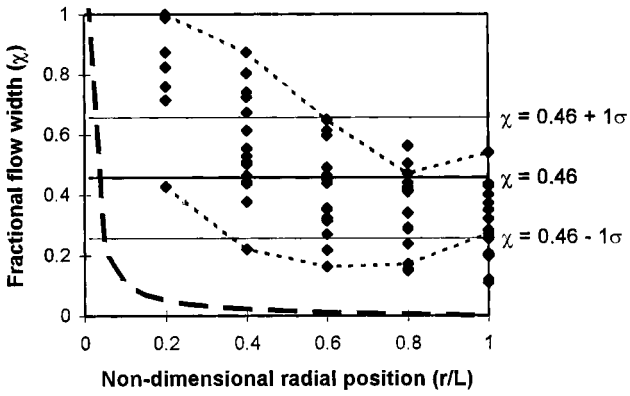

Figure 10. Variation in fractional flow width (χ) as a function of non-dimensional radial position (r/L) observed over a 75 min interval (recorded every 5 min) during run S10 (Q_w = 465 cm^{3}s^{-1}, Q_{so} = 7.55 cm^{3}s^{-1}, D = 120 μm). Time lines are shown (thin dash) for two representative realizations of down-fan patterns. Heavy dashed line shows theoretical "equilibrium" channel model (equation 2a). Solid lines show (1) best-fit "expanding flow" model (medium solid line) and (2) upper and lower bounds (thin solid lines) for the "expanding flow" fit.

inundation widths (χ) as a function of radial position ($\hat{r}$), document the dramatic temporal fluctuations described above (figure 10) and demonstrate that observed flow configurations represent a combination of channelized and localized sheetflood components. The data in figure 10 have a significant weakness, however; the data document only the total width of inundation without regard for flow depth. As the theoretical model is structured around the ''effective'' width of channels, direct comparison between observed and predicted channel widths requires care.

The non-linearity of sediment transport is such that the bulk of sediment transport is accomplished by the deeper channels. Paola (1996) has shown how knowledge of the distribution of flow depths and velocities can be used to calculate the total sediment transport, and thereby derive an effective sediment transport coefficient (α_s) that produces the correct total sediment transport based on the average channel. This formulation is utilized in the one-dimensional theoretical model (Parker et al. 1998*a,* 1998*b*). Unfortunately it was not possible to acquire the required depth-velocity data for flows on the experimental fans; only an approximate characterization of the effective channel configuration is possible.

Although experimental flow width data do not readily fit either end-member channel model (expanding flow or equilibrium channels), one distinctive characteristic of all experimental flows helps to clarify the situation: with shallow overbank flows occurring on all parts of the fan and the deepest channels restricted to the uppermost fan, variability in flow depth consistently diminished rapidly down fan. Thus, we may expect a measure of total flow width to overestimate (perhaps greatly) ''effective'' channel width near the fan apex, but for this measure to improve steadily down fan. We can conclude that the simple expanding flow ($B_{ac} = \chi\theta r$) model: (1) better approximates observed flow configuration data, and (2) crudely accounts for the down-fan trend of decreased variability in flow depth (figure 10). Moreover, deposition consistently occurred in zones of rapid flow expansion (lobes). For these reasons, the expanding flow solution is used below in all comparisons of theory and observation. It is noteworthy that direct application of either the equilibrium channel model or diffusion-type sedimentation models (e.g., Begin 1988; Flemings and Jordan 1989; Paola et al. 1992) is not expected to correctly predict experimental results.

Total flow widths were determined from photographic and video data collected during experimental runs S9, S10, S12, and S13, covering both suspension-dominated and bedload dominated conditions, and variations in both water discharge and sediment feed rate. Simple time averages of fractional flow width data (e.g., expanding flow ''fit'' on figure 10) were used to characterize χ as a function of controlling variables (figure 11*a,* 11*b*). Error bars on figures 11*a* and 11*b* represent the scatter in measured total flow width at different times and at different positions on the fan. In all cases (including qualitative observations in all other experiments) fractional flow width χ varied linearly with water discharge Q_w (figure 11*a*). Conversely, fractional flow width was found to be independent of sediment feed rate Q_{so} (figure 11*b*). Notably, the equilibrium channel closure model predicts the opposite: that effective channel width is independent of water discharge but sensitive to sediment feed rate (equation 2), further supporting our conclusion that the experimental fans were effectively ''expanding flow'' fans. Finally, the data in figure 11 illustrate that in experiments with sediment finer than 160 μm, grain size affected fractional flow widths, with greater channelization in the finer-grained material. Qualitative observations during experiments with sediment finer than 120 μm confirm that increasingly fine sediment had the effect of progressively enhancing flow channelization. We interpret this effect as being in part due to the onset of significant suspended sediment transport, and in part due to the effective cohesion of channel banks cut into fine sediment; that is, part real, and part scale, effect.

Fan Profiles and Average Depositional Slope. Model predictions were tested against experimental observation using the above constraints on flow channelization. Model parameters were determined from either well-established empirical relations (sediment transport parameters α_s, n, and τ_c^*; hydraulic resistance parameters α_r and p) or direct observation (χ). With only one exception (α_s for the crushed coal experiments), no ''tuning'' of model parameters was done. Calculations presented below (using equation 1) allow (1) direct comparison of theoretical and measured radial profiles and (2) comparison of predicted and observed relationships between average fan slope and input conditions (Q_w, Q_{so}, D). Recall that average fan slopes were derived via least squares regression through truncated, averaged radial elevation profiles. This method effectively measures the mid-fan slope. To derive comparable slope estimates, the average slope of the central 20% of computed theoretical profiles was determined. The resulting average slope estimate corresponds well with that derived through linear regression of computed profiles; the

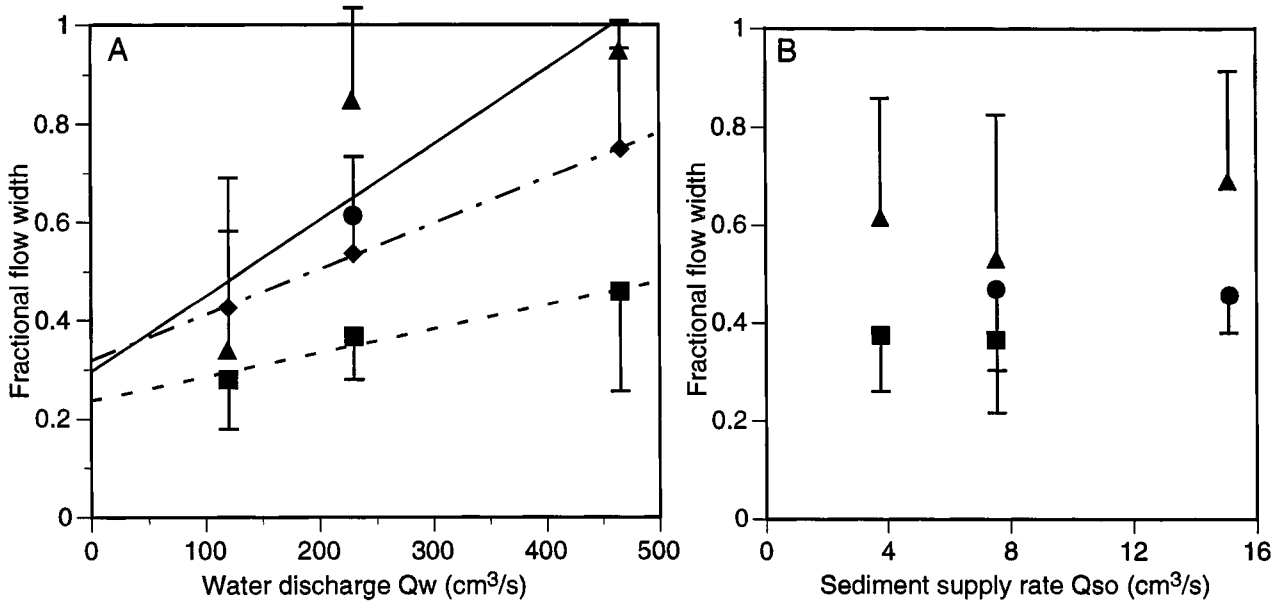

Figure 11. *A.* Best-fit fractional flow width (χ) values as a function of Q_w and D for runs S9, S10, S12, S13. Error bars represent scatter in total flow width data (see figure 10). For readability only half error bars are plotted. Symbols for data series: 460 μm (diamonds); 270 μm (triangles); 160 μm (circles); 120 μm (squares). Lines show best-fit trends determined by linear regression of the averaged data. These relationships are used in theoretical calculations (see table 2). *B.* Best-fit fractional flow width (χ) values as a function of Q_{so} and D for runs S9, S10. Symbols for data series: 160 μm, Q_w = 230 cm^3/s (triangles); 120 μm, Q_w = 465 cm^3/s (circles); 120 μm, Q_w = 230 cm^3/s (squares).

average mid-fan slope method was chosen as a matter of convenience. Results are insensitive to the exact methodology used to estimate average fan slope.

Model parameters used in the calculations are listed in table 2. In all cases, hydraulic resistance parameters α_r and p were determined from the Manning-Strickler relation

$$\frac{U}{u_*} = 8.1\left(\frac{H}{2.5D}\right)^{1/6}, \qquad (3)$$

and the critical Shields stress τ_c^* was determined according to the method of Brownlie (1981). For bedload-dominated sand systems, sediment transport parameters α_s and n were taken from the well-known Meyer-Peter-Mueller (1948) relation. For suspension-dominated sand systems, power-law regressions fit to empirical relations due to van Rijn (1984*a*, 1984*b*) were used to determine appropriate values of sediment transport parameters α_s and n. In this analysis suspended sediment loads were calculated with the van Rijn relations, using experimental conditions (D, σ_g, R, ν, S) as input. Sediment

Table 2. Model Parameters

Sediment Size (μm)	Hydraulic Resistence		Sediment Transport			Density	Channelization
D	α_r	p	α_s	n	τ_{cr}^*	R	χ
70	6.95	.167	16	1.8	.132	1.65	$500Q_w$ (m^3/s) + .237
120	6.95	.167	16	1.8	.081	1.65	$500Q_w$ (m^3/s) + .237
160	6.95	.167	16	1.8	.063	1.65	$1300Q_w$ (m^3/s) + .247
270	6.95	.167	8	1.5	.042	1.65	$1300Q_w$ (m^3/s) + .247
460	6.95	.167	8	1.5	.033	1.65	$1300Q_w$ (m^3/s) + .247
550	6.95	.167	8	1.5	.032	1.65	$1300Q_w$ (m^3/s) + .247
130	6.95	.167	14	2.0	.117	.38	$500Q_w$ (m^3/s) + .237
550	6.95	.167	4	1.5	.035	.50	$1300Q_w$ (m^3/s) + .247

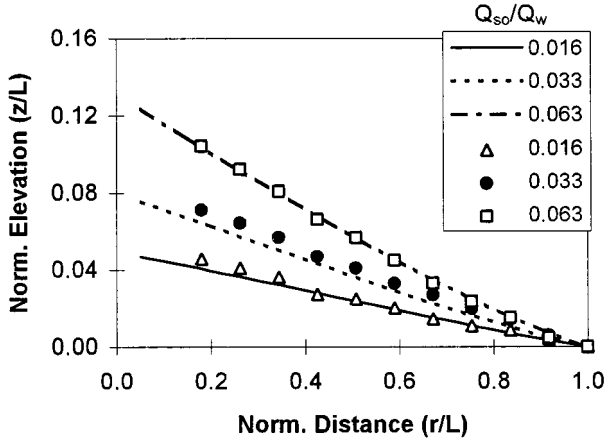

Figure 12. Predicted (lines) and observed (symbols) topographic profiles of a bedload-dominated fan (Run S12). Note the straight to gently concave profile form captured in the experiments and in theoretical predictions.

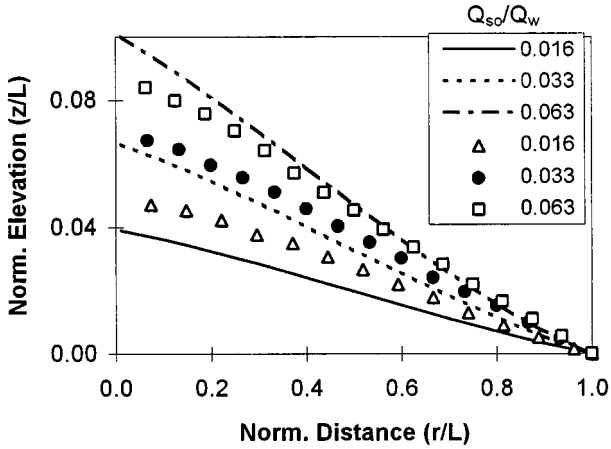

Figure 13. Predicted (lines) and observed (symbols) topographic profiles of a suspension-dominated fan (Run S10). Note the striking convexo-concave profile form captured in the experiments and in theoretical predictions.

transport rates were calculated for flow depths ranging from that observed in shallow overbank flows (1 mm) to the deepest channels (3 cm). Computed relations of sediment transport as a function of shear stress are approximated well by the generalized power-law transport relation used in the theoretical development (Parker et al. 1998*a*), with exponents n in the range of 1.8–2.2 and regression r^2 values typically in excess of 0.99. Computed transport relations for sand and silt mixtures are comparable to the well-known Engelund and Hansen relation (Engelund and Hansen 1967; $n = 2.5$). Inadequate information on the transport of angular, platy crushed coal shards and lack of quantitative information on flow channelization in the crushed coal experiments forced us to treat the sediment transport coefficient α_s as a fitting parameter for these experiments. We assume that the finding that the exponent n is about 1.5 for bedload transport and about 2.0–2.5 for suspended load transport is robust (Parker et al. 1998*a,* 1998*b*).

Direct comparison of theoretical prediction and experimental observation yields mixed results: the model performs well for the bedload-dominated sand fans (Series 3, table 1) and for the crushed coal fans (both suspension- and bedload-dominated systems; Series 4 and 5, table 1), but less well for the suspension-dominated sand fans (Series 1 and 2, table 1). Model predictions successfully capture many aspects of the bedload-dominated sand experiments: radial elevation profiles are straight to slightly convex (figure 12); fan slope decreases rapidly with increasing water discharge (figure 8*a*) and less rapidly with decreasing sediment supply rate (figure 8*b*); fan slope is independent of sediment size (figure 8*a*). Similarly, the theoretical model captures the essential behavior of the crushed coal systems: predicted relations between sediment concentration (Q_{so}/Q_w) and (relative) fan slope closely match observed relations in all cases (figure 9). As the sediment transport coefficient was "tuned" to the coal-fan data, only the model's success in predicting *trends* in slope-sediment concentration relationships is meaningful. However, it is significant that the *relative* rate of fan slope increase with sediment concentration is successfully predicted, regardless of sediment size or how the sediment concentration was varied. In this regard it should be noted that changing the Q_{so}/Q_w ratio produces a different response depending on (1) the dominant mode of sediment transport, and (2) whether Q_w or Q_{so} is varied.

Model predictions are less successful in the case of suspension-dominated sand experiments. Although predicted fan slopes are in the right range and the convexo-concave shape of radial profiles is well captured (figure 13), the rate of slope increase with sediment concentration is over-predicted in all cases (figure 6*a, b*). In addition, the grain size dependence observed in these experiments is much stronger than that expected from theory (equation 1; figure 6*a*). Note, however, that the decrease in slope between 160 and 120 μm is well modeled while that between 120 and 70 μm is not. This circumstance is easily explained: data used to quantify flow channelization in the 160 and 120 μm experiments are not available for the 70 μm experiments. Despite qualitative observations that flows were more effectively channelized in the 70

μm experiments, the channelization data for the 120 μm experiments were used in the calculations (table 2). Exploratory calculations indicate that reasonable estimates of fractional channel width (χ = .15–.25) for the 70 μm experiments yield approximately correct fan slopes; the observed grain size dependence can be inferred to derive mostly from differences in flow channelization.

Discussion

Theory and Observation. A simple model of alluvial fan sedimentation (Parker et al. 1998*a*) has been shown to describe adequately much of the behavior of experimental fans. The model's success in predicting observed relationships between sediment concentration, grain size, and fan slope for both the bedload-dominated sand experiments (figure 8) and the suspension- to bedload-dominated crushed coal experiments (figure 9) suggests that scaling problems may be responsible for the model's poorer performance in the case of the suspension-dominated sand experiments. This interpretation is further supported by the model's success in predicting the convex-concave radial profiles of the suspension-dominated fans, so capturing one of the important observed differences between the bedload- and suspension-dominated fans (figure 13). An opposing argument that the model's poor performance on the suspension-dominated sand experiment reflects an over-simplified treatment of the channel closure problem (exposed in our most extensive experiments involving significant flow channelization), however, cannot be entirely refuted. The strongest evidence against this argument is the successful prediction of slope-sediment concentration *trends* in the suspension-dominated crushed coal experiments (figure 9). This raises the question: why should scaling problems have been more exaggerated in the fine sand and silt experiments? A brief consideration of the nature of the scaling problems holds a plausible answer.

Scale issues are associated with low Reynolds numbers, effective cohesion of fine sediment, and incorrect geometric scaling. Potential scale effects include: (1) reduced Reynolds numbers resulting in suppression of particle suspension in thin overbank flows and precluding proper scaling of bedforms; (2) effective bank cohesion due to capillary tension in fine-grained model sediments affecting channelization processes; and (3) incorrect scaling of individual channel-lobe couplets, potentially exaggerating the importance of rapidly expanding flows in the experiments. Of these, deviations from Reynolds similarity are the only scale effect that may arguably differ between the sand-silt and crushed coal experiments. We suggest that despite low Reynolds numbers, suspension of crushed coal particles was not significantly suppressed in our experiments (unlike the case for sand-silt particles). Inlet flows were always highly turbulent and all fine sediments entered the fan in suspension. As crushed coal particles settle far more slowly than quartz sand grains of the same size, they only fall out of suspension at much lower Reynolds numbers and after much longer transport distances than denser sand-silt grains. It thus seems reasonable to infer that the Reynolds-scaling problems described below were less important in the crushed coal experiments.

Fan-head Trenching. In our experiments, as in those reported by Schumm et al. (1987), spontaneous periodic episodes of fan-head trenching were observed to occur under a wide range of experimental conditions (e.g., figure 3 and 4). Schumm et al. (1987) were able to demonstrate that their fan-head trenching episodes were not driven by fluctuations in sediment load or water discharge but rather seemed to be related to a channel incision threshold. Our observations of episodic fan-head entrenchment under steady input conditions confirm this interpretation. However, careful consideration of processes operative under experimental conditions suggests the possibility that the observed behavior is scale-dependent.

Reduced flow Reynolds numbers and exaggerated geometric scaling relationships between the fan landform and individual morphological elements (bedforms, individual channels, and midchannel bars) appear to play important, perhaps dominant, roles in the observed episodic fan-head trenching. Sudden channelization, dramatic fluctuations of channel bed profiles, and fan-head trenching were most pronounced on suspension-dominated fans where abrupt transitions between bedload transport in thin overbank sheetflows and vigorous suspension in channels occur and seem to be associated with a threshold slope for channel initiation, as described by Schumm et al. (1987). This threshold for channel incision, however, may well not scale correctly with the field phenomenon; whereas bedload-dominated sheetflows effectively scale as gravel-bedded systems, suspension-dominated channel flows effectively scale as sand and granule-bedded systems (see Appendix A), thus dramatically exaggerating the suddenness and depth of channel entrenchment. The same processes are

likely to have been operating on the fluvial fans studied by Schumm et al. (1987): the fine-grained sediment, high water discharges, and moderate slopes of their experimental fans are consistent with a suspension-dominated system similar to our run series 1 and 2 experiments. Autocyclic fan-head entrenchment on our experimental fans cannot be confidently extrapolated to field scale.

Channelization: Braided Channels or Sheetflows. It should be noted that comparison with theory required the empirical evaluation of a parameter associated with partial sheet flow, i.e. χ, that is not predicted from theory. The necessity to treat the flows on the model fans as expanding flows rather than channelized flows may be in part a scale effect. That is, if either fan length or fan width is not sufficiently large compared with the characteristic width of a channel, the effect of channelization on gross fan morphology may not become fully established in the experiments. Another factor is the very large effective discharge used in the experiments. These issues could be addressed in future by simply using a larger experimental facility.

Despite the small size of the experimental facility, flows on the experimental fans were fundamentally channelized: zones of expanding flow were unstable and were observed to rapidly break down into multiple-thread, crudely braided channels. Transient and spatially restricted channels formed rapidly, entrenched, backfilled and avulsed frequently, sweeping across and regarding the fan surface (figures 3–5). As noted above, however, the sedimentation dynamics appear to have been dominated by the rapidly expanding flows that disperse sediment to depositional lobes at the distal ends of the channels. This inference is corroborated by the success of the ''expanding flow'' theoretical model in predicting the slopes and radial profiles of the experimental fans. It is tempting to conclude that field scale gravel bedded alluvial fans, such as those in Death Valley, California, are indeed sheetflood-dominated fans, as argued by some researchers (Blair 1987; Blair and McPherson 1994). However, the importance of rapidly expanding ''sheetfloods'' is likely exaggerated by the restricted basin size of the experiments. First, the experimental flow discharges scale as very high magnitude flood events (100–400 m^3/s) on very small fans ($L = 500$ m). Second, the physical scale of individual channel-lobe couplets is seriously out of proportion on the experimental fans: features that might scale as mid-channel bars in the field at times occupy as much as one third of the experimental fans, potentially making a fundamentally channelized flow mimic a sheetflood on the scale model. At present we cannot draw confident conclusions about the direct relevance of our experimental results to the controversy over the relative importance of sheetfloods and braided channel flows on natural alluvial fans. However, the experimental data provide an important proving ground for a theoretical model more suited to extrapolation to field scale. Moreover, our findings highlight the need for field studies of alluvial fan hydraulics and should provide a useful guide for them.

Conclusions

A comprehensive suite of experiments on alluvial fan sedimentation was carried out to determine the relationship between fan slope and water discharge Q_w, sediment supply rate Q_{so}, and sediment size D. Experimental observations were limited to the idealized case of constant inflow conditions in part to isolate intrinsic controls on fan slope (independent of any external forcings) and in part to allow us to test a simple theoretical model of fan evolution (Parker et al. 1998*a*). An imposed constantly rising base level allowed fan deposition to be observed under a state of nearly steady, uniform aggradation, mimicking a long-term balance between sedimentation and subsidence. The matrix of experimental conditions was fairly extensive, covering a wide range of water discharges (108–475 cm^3s^{-1}), sediment supply rates (1.73–15.09 cm^3s^{-1}), particle sizes (70–550 μm), and both bedload-dominated and suspension-dominated fans.

The degree of flow channelization was found to have an important influence on sedimentation patterns, dynamics, and the resulting equilibrium depositional slope. Flows invariably consisted of a combination of rapidly avulsing channels and localized sheetfloods, with the degree of channelization dependent upon water discharge and grain size, but independent of sediment supply. This channelization behavior cannot be explained with existing equilibrium or threshold channel closure rules commonly used in large-scale sedimentation models (e.g., Paola et al. 1992). The ''expanding flow'' version of the theoretical model (Parker et al. 1998*a*) was remarkably successful at predicting observed relationships between fan slope, grain size, and sediment concentration. This ''sheetflood-like'' behavior cannot, however, be directly extended to field scale, as it is likely due in part to the small size of the experimental facility compared to channel scale. Rather, the model's success at reproducing experimental observations

is taken as direct evidence that the theoretical model has some merit. Extrapolation to field scale is better done by judicious application of the theoretical model than by direct extension of experimental observations. Further, several scale issues associated with reduced Reynolds numbers, physical size of the model fans, and effective cohesion of fine model sediments must be considered in the extrapolation of experimental findings to field scale.

ACKNOWLEDGMENTS

This research was funded by the Hibbing Taconite Company and the National Science Foundation (Grants no. CTS-9207882 and CTS-9424507). The paper benefited from comments by R. French and an anonymous reviewer. Sameer Kirtane digitized still and video images of flow configuration. Many of the initial experiments were performed by John Ahern. His help, as well as the help of Carlos Toro-Escobar is gratefully acknowledged.

REFERENCES CITED

Begin, Z. B., 1988, Application of a diffusion-erosion model to alluvial channels which degrade due to base-level lowering: Earth Surf. Proc. Landforms, v. 13, p. 487–500.

Blair, T. C., 1987, Sedimentary processes, vertical stratification sequences, and geomorphology of the Roaring River alluvial fan, Rocky Mountain National Park, Colorado: Jour. Sed. Pet., v. 57, p. 1–18.

———, and McPherson, J. G., 1994, Alluvial fans and their natural distinction from rivers based on morphology, hydraulic processes, sedimentary processes, and facies assemblages: Jour. Sed. Res., v. A64, p. 450–489.

Blissenbach, E., 1954, Geology of alluvial fans in semiarid regions: Geol. Soc. America Bull., v. 65, p. 175–190.

Brownlie, W. R., 1981, Prediction of flow depth and sediment discharge in open channels: Keck Laboratory, California Inst. Tech. Rept. KH-R-43A, 232 p.

Bryant, M.; Falk, P.; and Paola, C., 1995, Experimental study of avulsion frequency and rate of deposition:Geology, v. 23, p. 365–368.

Bull, W. B., 1977, The alluvial fan environment: Prog. Phys. Geog., v. 1, p. 222–270.

Denny, C. S., 1965, Alluvial fans in the Death Valley Region, California and Nevada: U.S. Geol. Survey Prof. Paper 466, p. 1–62.

Dietrich, W. E., 1982, Settling velocity of natural particles: Water Resour. Res., v. 18, p. 1615–1626.

Engelund, F., and Hansen, E., 1967, A Monograph on Sediment Transport in Alluvial Streams: Copenhagen, Denmark, Teknisk Forlag, 62 p.

Flemings, P. B., and Jordan, T. E., 1989, A synthetic stratigraphic model of foreland basin development: Jour. Geophys. Res., v. B94, p. 3851–3866.

French, R. H., 1985, Open-Channel Hydraulics: New York, McGraw-Hill, 705 p.

———, 1992, Preferred directions of flow on alluvial fans: Jour. Hydr. Eng., v. 118, p. 1002–1013.

Gordon, I., and Heller, P. L., 1993, Evaluating major controls on basinal stratigraphy, Pine Valley, Nevada: Implications for syntectonic deposition: Geol. Soc. America Bull., v. 105, p. 47–55.

Graf, W. H., 1977, Hydraulics of Sediment Transport: New York, McGraw-Hill, 513 p.

Hooke, R. L., 1967, Processes on arid-region alluvial fans: Jour. Geology, v. 75, p. 438–460.

———, 1968, Steady-state relationships on arid-region alluvial fans in closed basins: Am. Jour. Sci., v. 266, p. 609–629.

———, and Rohrer, W. L., 1979, Geometry of alluvial fans: Effect of discharge and sediment size: Earth Surf. Proc., v. 4, p. 147–166.

Izumi, N., and Parker, G., 1995, Inception of channelization and drainage basin formation: Upstream-driven theory: Jour. Fluid Mech., v. 283, p. 341–363.

Loewenherz-Lawrence, D. S., 1994, Hydrodynamic description for advective sediment transport processes and rill initiation: Water Resour. Res., v. 30, p. 3203–3212.

Meyer-Peter, E., and Mueller, R., 1948, Formulas for bed-load transport: Proc. Second Congress: Stockholm, Int. Assoc. Hydraul. Structures Res., p. 39–64.

Nilsen, T. H., and Moore, T. E., 1984, Bibliography of Alluvial-Fan Deposits: Norwich, UK, Geo Books, 96 p.

Paola, C., 1996, Incoherent structure: Turbulence as a metaphor for stream braiding, *in* Ashworth, P. J.; Bennett, S. J.; et al., eds., Coherent Flow Structures in Open Channels: Chichester, Wiley, p. 705–723.

Paola, C.; Heller, P. L.; and Angevine, C. L., 1992, The large-scale dynamics of grain-size variation in alluvial basins, 1: Theory: Basin Res., v. 4, p. 73–90.

Parker, G., 1978*a,* Self-formed straight rivers with equilibrium banks and mobile bed. Part II. The gravel river: Jour. Fluid Mech., v. 89, p. 127–148.

———, 1978*b,* Self-formed straight rivers with equilibrium banks and mobile bed. Part I. The sand-silt river: Jour. Fluid Mech., v. 89, p. 109–125.

———; Paola, C.; Whipple, K. X.; and Mohrig, D., 1998*a,* Fluvial Fans: Theory: Jour. Hydr. Eng., v. 124, n. 10, p. 1–11.

———; Paola, C.; Whipple, K. X.; Mohrig, D.; Toro-Escobar, C. M.; Ruffner, R.; and Halvorsen, M., 1998*b,* Fluvial fans: Application: Jour. Hydr. Engin., v. 124, n. 10, p. 12–20.

Price, W. E., 1976, A random-walk simulation of alluvial-fan deposition, *in* Merriam, D. F., ed., Random Processes in Geology: New York, Springer-Verlag, p. 55–62.

Rachochi, A., 1981, Alluvial Fans: New York, Wiley, 161 p.

Schumm, S. A.; Mosley, P. M.; and Weaver, W. E., 1987, Experimental Fluvial Geomorphology: New York, Wiley, 413 p.

Smith, T. R., and Bretherton, F. P., 1972, Stability and the conservation of mass in drainage basin evolution: Water Resour. Res., v. 8, p. 1506–1529.

van Rijn, L. C., 1984*a,* Sediment transport, part I: Bed load transport: Jour. Hydr. Eng., v. 110, p. 1431–1456.

———, 1984*b,* Sediment transport, part II: Suspended load transport: Jour. Hydr. Eng., v. 110, p. 1613–1641.

Whipple, K. X., and Trayler, C., 1996, Tectonic controls on fan size: the importance of spatially variable subsidence rates: Basin Res., v. 8, p. 351–366.

Appendix A: Model-Prototype Scaling Relations

Perfect scale models of natural fluvial systems are generally impossible to achieve. This is partly because both Froude and Reynolds similarity can rarely be achieved in tandem, and partly because fine cohesive sediment typically provides a poor scale model of larger non-cohesive sediment. The first problem can be partially circumvented by operating in a range within which Reynolds effects on resistance and sediment transport are not too strong. The second can be circumvented by the use of non-cohesive sediment in the model.

In modeling bedload-dominated fluvial systems, it is generally acceptable to relax Reynolds similarity as long as flow remains turbulent, while imposing strict Froude and Shields number similarity (French 1985; Graf 1977). Reynolds similarity becomes more important in modeling suspension-dominated systems, where turbulence plays an essential role in sediment transport dynamics. In these systems an approach is to impose similarity in the Froude and Rouse numbers, the latter being related to Reynolds number, while partially relaxing Shields similarity. An implication is that model-prototype relations in suspension-dominated systems differ from those of bedload-dominated systems.

Scale Models with Sand and Silt. For an undistorted scale model imposing Froude and Shields similarity, and employing sediment with the same specific gravity ρ_s/ρ as the prototype, the ratio of model to prototype vertical scales H_r must be equal to the corresponding horizontal scale ratio L_r. In addition, the grain size ratio D_r, and velocity ratio U_r, and discharge ratio Q_r of water or sediment must satisfy the following relations between model and prototype (French 1985; Graf 1977):

$$D_r = L_r = H_r; \qquad U_r = L_r^{1/2}; \qquad Q_r = L_r^{5/2}. \qquad \text{(A1a,b,c)}$$

For suspension-dominated systems, the appropriate scaling relationships must impose primarily Froude and Rouse number similarity. In this case the relevant scaling relationships are:

$$L_r = H_r; \qquad U_r = L_r^{1/2}; \qquad Q_r = L_r^{5/2}; \qquad W_{sr} = Lr^{1/2} \qquad \text{(A2a,b,c,d)}$$

where W_{sr} is the ratio of model to prototype fall velocities. For a given particle shape, dimensionless particle fall velocity $w_s/\sqrt{\boldsymbol{R}gD}$ can be uniquely related to a particle Reynolds number $\boldsymbol{Re}_p = \sqrt{\boldsymbol{R}gD}\, D/\nu$ (Dietrich 1982; Parker 1978b). The appropriate grain size scaling

ratio D_r is constrained by equation (A2d) and can be determined iteratively using the equations presented by Dietrich (1982). Note that in this case the condition $D_r > L_r$ holds, implying a different grain-size relationship between model and prototype than in the bedload dominated case.

Scale Models with Crushed Coal. In scale models of relatively fine-grained systems (e.g., sand to granule particle sizes) it is often necessary to utilize a model sediment with a lower specific gravity than the prototype sediment (French 1985; Graf 1977). Such models are necessarily distorted models; that is the horizontal, vertical, and sediment size scale ratios are no longer equal. Using a low-density model sediment such as crushed coal, Froude and both Shields and Rouse similarity can be (approximately) achieved simultaneously in a vertically exaggerated model. In this case the relevant scaling relationships are:

$$H_r = \left(\mathbf{R}_r D_r L_r\right)^{1/2}; \quad U_r = H_r^{1/2}; \quad Q_r = H_r^{3/2} L_r; \quad W_{sr} = H_r L r^{-1/2}, \quad \text{(A3a,b,c,d)}$$

where D_r is constrained by (A3d) and equations in Dietrich (1982), and H_r is derived from (A3a). It is worth noting that although the relative roughness (D/H) is enhanced in such vertically exaggerated models, it is easily shown that this actually compensates for reduced model Reynolds numbers and helps to preserve similarity in the effective hydraulic roughness.